Backprojection Autofocus of Moving Ships for Synthetic Aperture Radar

Aron Sommer#1, Jörn Ostermann#2
#Institut für Informationsverarbeitung,
Leibniz Universität Hannover, Germany
1sommer@tnt.uni-hannover.de, 2ostermann@tnt.uni-hannover.de

***Abstract*— In this paper, we present a backprojection autofocus method to image moving ships in high resolution very precisely. This technique might make an automatic ship classification based on Synthetic Aperture Radar (SAR) images without using additional information from the Automated Identification System (AIS) possible. We use a Constant False Alarm Rate (CFAR) detector to estimate the coarse position of a ship in a preview SAR image. A second high resolution image of the ship is generated by the proposed backprojection autofocus algorithm. Our autofocus estimates the time depending distance between the sensor and every pixel in the SAR image, which includes the rotation and the translation of the ship. This estimated relative distance is used to compute a high quality autofocused SAR image of the considered moving ship.**

***Keywords*— Synthetic aperture radar, inverse synthetic aperture radar, airborne radar, radar detection, radar imaging, autofocus.**

I. Introduction

Ship detection and identification plays an important role in maritime surveillance. It allows monitoring of maritime traffic, boarder control and illegal activities. Usually spaceborne or airborne Synthetic Aperture Radar (SAR) systems are used to detect ships in radar images of the sea surface with wide-area coverage in all-weather as well as day/night conditions. Optical sensors do not offer a wide area overview together with high resolution in far range simultaneously. Hence, the technique of SAR is well suited to detect ships at sea [1].

The Automated Identification System (AIS) is a wireless broadcast technology, where marine objects send information about their identity, their position and their destination using radio frequencies. Thus, the combination of SAR as a detection algorithm and AIS for the identification part is widely used for detection and identification of ships on the open sea [2].

However, AIS is only useful if legal marine objects are monitored. It is conceivable that illegal ships could turn off their AIS system or could send fake information, which make an identification impossible. Without reliable AIS information, ships can only be detected, because SAR without autofocus techniques offers not the necessary image quality to identify or even classify marine objects. The problem is that ships appear shifted and smeared in radar images due to their motion during the long radar evaluation time of several seconds. Thus, a ship can be detected, but it can rarely be identified.

Several autofocus techniques have been investigated to improve the image quality by estimating small motion deviations of the platform or of the moving object, respectively. One state-of-the-art autofocus algorithm is the Backprojection Autofocus from Duersch et al. [3] with the extension from Ash [4]. It has the capability of focusing moving ships and will be discussed later in detail. Livingstone et al. [1] estimate sine and cosine motions of a ship in frequency domain, which result in improvements of the SAR image quality.

In this paper we propose an autofocus technique to image moving ships with high quality. This technique uses the Backprojection algorithm [5] together with an integrated autofocus. We extract information of prominent point reflectors on a ship to estimate its real motion. This estimated motion is used to generate a precisely focused SAR image of the moving ship, which is sharper than images processed by standard autofocus techniques.

The structure of this paper is as follows: Section II introduces the signal model and presents how simulated data is generated. The impact of ship motion on data and the problem formulation is given in Section III. A state-of-the-art autofocus is described in Section IV. The proposed autofocus method is presented in Section V. In Section VI the results of our algorithm, applying it to synthetic data of a simulated tanker, are shown. This paper ends with conclusions in Section VII.

II. Signal Model

Let an aircraft carry a single-channel SAR system. It flies along an arbitrary flight path $\gamma : \mathcal{L} \to \mathbb{R}^3$, which is described in global coordinates and parametrized by slow-time $s \in \mathcal{L}$ with $\mathcal{L} := [0, T_\mathrm{a}]$. The SAR integration time $T_\mathrm{a} \in \mathbb{R}$ corresponds to the synthetic aperture length. Let the antenna transmits the chirp pulse [7]

$$p(t) = \mathrm{rect}(\tfrac{t}{T}) \exp(-2\pi \mathrm{i} f_\mathrm{c} t) \exp(\mathrm{i}\pi\kappa t^2), \quad t \in \mathcal{T},$$

where f_c is the carrier frequency, $\kappa = B/T$ the chirp rate, B the chirp bandwidth and T the pulse duration. This electromagnetic wave p is transmitted by the antenna, scattered at some objects in the illuminated area Ω on the ground and received by the antenna within the sampling time interval $\mathcal{T}$, also known as fast-time interval. The receiver measures the echo

$$p_r(t) = \mathrm{rect}(\tfrac{t-\tau}{T}) \exp(-2\pi \mathrm{i} f_\mathrm{c}(t-\tau)) \exp(\mathrm{i}\pi\kappa(t-\tau)^2), \quad (1)$$

for $t \in \mathcal{T}$, where $\tau = 2\,r/c$ describes the two way round trip time for a single point scatterer.

We assume that $\Omega \subset \mathbb{R}^3$, especially each $\boldsymbol{x} \in \Omega$ represents the coordinates of the scene. The reflectivity, which includes the ships and the waves, is modeled by a time dependent complex reflectivity function $\mathcal{V} : \Omega \times \mathcal{L} \to \mathbb{C}$ of the illuminated area. Hence, the value of the reflectivity function $\mathcal{V}$ at $\boldsymbol{x}$ depends on the motion of a marine object with slow-time s. Thus, the raw data, which is in principle the superposition of the echos in Eq. (1) from many point reflectors, reads

$$d_{\text{raw}}(t,s) = \int\limits_{\Omega} A(\boldsymbol{x},s)\,\mathcal{V}(\boldsymbol{x},s) \cdot p\Big(t - \tfrac{2\,||\,\boldsymbol{\gamma}(s)-\boldsymbol{x}||}{c}\Big)\,\mathrm{d}\boldsymbol{x} \tag{2}$$

for $t \in \mathcal{T}$, $s \in \mathcal{L}$, speed of light c and antenna beam pattern A. Eq. (2) is derived from the signal model given by Cheney [6]. The raw data d_{raw} is then matched filtered and results in the range compressed data [7]

$$\begin{aligned} d(t,s) &= d_{\text{raw}}(t,s) * p^*(-t) \\ &\approx \int\limits_{\Omega} A(\boldsymbol{x},s)\,\mathcal{V}(\boldsymbol{x},s)\ \mathrm{si}\Big(\pi\kappa T\Big(t - \tfrac{2\,||\,\boldsymbol{\gamma}(s)-\boldsymbol{x}||}{c}\Big)\Big) \\ &\quad \cdot \exp\Big(-2\pi\mathrm{i} f_{\mathrm{c}} \tfrac{2\,||\,\boldsymbol{\gamma}(s)-\boldsymbol{x}||}{c}\Big)\,\mathrm{d}\boldsymbol{x} \end{aligned} \tag{3}$$

for $t \in \mathcal{T}$ and $s \in \mathcal{L}$. The operation $*$ stands for the convolution and $\cdot^*$ is the complex conjugation. In the next part we consider the impact of ship motion on data d.

III. Impact of Ship Motion

In this section we draw our attention to the analysis of the range compressed data of a single ship. The derived formulation at the end of this chapter is one of the novelties given in this paper. Let the guard area $\mathcal{M} \subset \Omega$ of a ship be the ship itself and its near surrounding. We assume that the ship is illuminated only during the ship integration time $\mathcal{L}_0 \subset \mathcal{L}$. Hence, we model the antenna beam $A(s,\boldsymbol{x})$ as a binary function constant in time $s \in \mathcal{L}_0$ and space $\boldsymbol{x} \in \mathcal{M}$. Thus, we can neglect the antenna beam pattern and get the range compressed data

$$d(t,s) = \int\limits_{\mathcal{M}} \mathcal{V}(\boldsymbol{x},s)\ \mathrm{si}\Big(\pi\kappa T\Big(t - \tfrac{2\,||\,\boldsymbol{\gamma}(s)-\boldsymbol{x}||}{c}\Big)\Big) \cdot \exp\Big(-2\pi\mathrm{i} f_{\mathrm{c}} \tfrac{2\,||\,\boldsymbol{\gamma}(s)-\boldsymbol{x}||}{c}\Big)\,\mathrm{d}\boldsymbol{x}$$

for $s \in \mathcal{L}_0$ and $\boldsymbol{x} \in \mathcal{M}$ of a single ship. The ship moves in azimuth, range and height. It additionally turns around pitch, roll and yaw, which altogether are influenced by its velocity, its track and the sea waves. We denote the axes of the global coordinate system by x, y and z, where its origin lies at the ship center at time zero.

We assume that during the integration time $\mathcal{L}_0$ of one considered ship its reflectivity $\mathcal{V}$ does not depend on the aspect ratio angle. It depends on $\boldsymbol{x}$ and on its motion, especially on the rotation $R : \mathcal{L}_0 \to \mathbb{R}^{3\times 3}$ and on the translation $m : \mathcal{L}_0 \to \mathbb{R}^3$. Thus, the reflectivity $\mathcal{V}$ of a ship can be written by

$$\mathcal{V}(\boldsymbol{x},s) := \mathcal{V}_0\big(R(s)\cdot\boldsymbol{x} + m(s)\big),$$

where $\boldsymbol{x}$ is the coordinate and s the slow-time. A simple change of variables $\widetilde{\boldsymbol{x}} := R(s)\cdot\boldsymbol{x} + m(s)$ yields the approximated range compressed data

$$d(t,s) = \int\limits_{\mathcal{M}} \mathcal{V}_0(\widetilde{\boldsymbol{x}})\ \mathrm{si}\Big(\pi\kappa T\Big(t - \tfrac{2\,||\gamma(s)-R(s)\cdot\widetilde{\boldsymbol{x}}-m(s)||}{c}\Big)\Big) \cdot \exp\Big(-2\pi\mathrm{i} f_{\mathrm{c}} \tfrac{2\,||\,\boldsymbol{\gamma}(s)-R(s)\cdot\widetilde{\boldsymbol{x}}-m(s)||}{c}\Big)\,\mathrm{d}\widetilde{\boldsymbol{x}},$$

where $\mathcal{V}_0(\widetilde{\boldsymbol{x}})$ is now static over time $s \in \mathcal{L}_0$. This enables us to use the Backprojection algorithm [5] to generate a SAR image of the ship. From now on, we assume that the scene $\Omega \subset \mathbb{R}^3$ is a flat surface with height $z = 0$. The intensity image is computed by

$$\begin{aligned} I(\boldsymbol{x}) &= |\mathcal{V}_0(\boldsymbol{x})| \\ &= \Bigg|\int\limits_{\mathcal{L}_0} d\Big(\tfrac{2\,||\,\boldsymbol{\gamma}(s)-R(s)\cdot\boldsymbol{x}-m(s)||}{c}, s\Big) \\ &\quad \cdot \exp\Big(2\pi\mathrm{i} f_{\mathrm{c}} \tfrac{2\,||\,\boldsymbol{\gamma}(s)-R(s)\cdot\boldsymbol{x}-m(s)||}{c}\Big)\,\mathrm{d}s\Bigg|. \end{aligned}$$

Note that the intensity $I(\boldsymbol{x}) \in \mathbb{R}$ at $\boldsymbol{x} \in \mathbb{R}^3$ is the absolute value of the reflectivity $\mathcal{V}_0(\boldsymbol{x}) \in \mathbb{C}$. Hence, we look for the relative rotation R and the relative translation m between the aircraft and the ship, to get a focused image.

In far field, the movement of the ship can be approximated by a relative change of the distance

$$r_{\triangle}(\boldsymbol{x},s) = ||\,\boldsymbol{\gamma}(s) - R(s)\cdot\boldsymbol{x} - m(s)|| - ||\,\boldsymbol{\gamma}(s) - \boldsymbol{x}||$$

between sensor and every coordinate $\boldsymbol{x}$ of the flat ship:

$$\mathcal{V}_0(\boldsymbol{x}) \approx \int\limits_{\mathcal{L}_0} d\Big(\tfrac{2\,(||\,\boldsymbol{\gamma}(s)-\boldsymbol{x}||+r_{\triangle}(\boldsymbol{x},s))}{c}, s\Big) \cdot \exp\Big(2\pi\mathrm{i} f_{\mathrm{c}} \tfrac{2\,(||\,\boldsymbol{\gamma}(s)-\boldsymbol{x}||+r_{\triangle}(\boldsymbol{x},s))}{c}\Big)\,\mathrm{d}s. \tag{4}$$

Finally, the autofocus problem formulation of a moving ship reads as follows: Estimate the relative motion $r_{\triangle}$ between the sensor and every part of the ship, which depends on time and enables the calculation of a focused image of the ship by Backprojection. This statement is our first result of this paper. It is confirmed by the simulated results in Fig. 2a in Section VI. How the function $r_{\triangle}$ is estimated with a standard autofocus is described in the next section.

IV. State-of-the-Art Backprojection Autofocus

We compare our method, which is described in detail in Section V, with the backprojection autofocus algorithm from Duersch and Long [3] in combination with the extension from Ash [4]. The latter invented a closed-form solution of the so far iterative phase error calculation. Both make the assumption, that $r(\boldsymbol{x},s) \approx r(s)$ is constant over space and less than the range resolution of the SAR system. Thus, the relative motion

$r(\boldsymbol{x}, s)$ in Eq. (4) results in the phase error $\phi_\epsilon(s)$ so that the autofocus SAR reflectivity image is

$$\mathcal{V}_0(\boldsymbol{x}) \approx \int_{\mathcal{L}_0} d\Big(\tfrac{2\,||\boldsymbol{\gamma}(s)-\boldsymbol{x}||}{c}, s\Big) \cdot \exp\Big(2\pi \mathrm{i} f_\mathrm{c}\, \tfrac{2\,||\boldsymbol{\gamma}(s)-\boldsymbol{x}||}{c} + \mathrm{i}\,\phi_\epsilon(s)\Big)\, \mathrm{d}s.$$

The general idea of this autofocus method [3], [4] is to find for every pulse $d(t, s_m)$ with fixed $s_m \in \mathcal{L}_0$ the phase error $\phi_\epsilon(s_m)$, which yields a focused image. Thus, the algorithm estimates from pulse to pulse the phase correction

$$\widehat{\phi}_\epsilon(s_m) = \arg\max_{\phi} S_m(\widehat{\phi}_\epsilon(s_1), \ldots, \widehat{\phi}_\epsilon(s_{m-1}), \phi, \widehat{\phi}_\epsilon(s_{m+1}), \ldots, \widehat{\phi}_\epsilon(s_{N_\mathrm{az}}))$$

of the m-th pulse, which maximizes the *maximum contrast* sharpness cost function

$$S_m(\boldsymbol{\phi}) = -\sum_{i=1}^{N_\mathrm{pix}} |I_m(\boldsymbol{x}_i, \phi)|^2 \tag{5}$$

of the discrete formulated SAR intensity image

$$I_k(\boldsymbol{x}_n, \phi) = \sum_{\substack{m=1\\ m\neq k}}^{M} d_m\Big(\tfrac{2\,||\boldsymbol{\gamma}_m - \boldsymbol{x}_n||}{c}\Big) \exp\Big(2\pi \mathrm{i} f_\mathrm{c} \tfrac{2\,||\boldsymbol{\gamma}_m - \boldsymbol{x}_n||}{c}\Big) \cdot \exp\Big(-\mathrm{i}\widehat{\phi}_m\Big) + d_k\Big(\tfrac{2\,||\boldsymbol{\gamma}_k - \boldsymbol{x}_n||}{c}\Big) \cdot \exp\Big(2\pi \mathrm{i} f_\mathrm{c} \tfrac{2\,||\boldsymbol{\gamma}_k - \boldsymbol{x}_n||}{c}\Big) \exp\Big(-\mathrm{i}\phi\Big).$$

In other words, the Duersch and Ash autofocus technique varies sequentially the m-th pulse for $m = 1, \ldots, N_\mathrm{az}$, where all other pulses stay fixed, to find the estimation of the m-th phase error $\widehat{\phi}_\epsilon(s_m)$. The related image is computed by

$$\mathcal{V}_0(\boldsymbol{x}) = \int_{\mathcal{L}_0} d\Big(\tfrac{2\,||\boldsymbol{\gamma}(s)-\boldsymbol{x}||}{c}, s\Big) \cdot \exp\Big(2\pi \mathrm{i} f_\mathrm{c}\, \tfrac{2\,||\boldsymbol{\gamma}(s)-\boldsymbol{x}||}{c}\Big) \cdot \exp\Big(-\mathrm{i}\,\widehat{\phi}_\epsilon(s)\Big)\, \mathrm{d}s,$$

which shows the focused object. This autofocus is widely used for Backprojection and yields good results, if the motion error is less than the range resolution of the SAR system. However, moving objects including ships on the open sea usually move more than a few centimeter within the integration time of several seconds. This is the reason, why autofocus techniques have problems by focusing moving objects.

V. Proposed Ship autofocus technique

We assume that a ship detector estimates the coarse position of every ship based on a low resolution preview SAR image. This preview image can be generated by any SAR processing technique like Omega-K [7] or Fast Factorized Backprojection [8]. We use a standard Constant False Alarm Rate (CFAR) detector [9] to estimate the center position $\boldsymbol{x}_0$ of a ship. Note that the detection process is not the main topic of this paper.

Furthermore, we compute a static SAR image centered at $\boldsymbol{x}_0$ with a very short integration time t_0. In our scenario we use for example $t_0 = 0.05\,\mathrm{s}$. This image serves as a registration basis for all following pulses. This can be done, because within this short time interval, the ship does not move much. This image is also used to find prominent points, for example corner reflectors, at the ship. Again we use a CFAR detector to find the position of each prominent point. Based on these strong reflectors, we estimate their movement by a differential autofocus technique, which we describe in the following.

Let k be the index of each pulse, then the image of the local environment around one prominent point, generated by 10 pulses, is $\mathcal{V}_{10}$. Now the autofocus begins by the registration of the next pulse to the image. This is done by using Ash [4] for finding the phase error $\widehat{\phi}_k$. Thus the image of one point reflector is iteratively processed for $k > 10$ by

$$\widetilde{\mathcal{V}}_k(\boldsymbol{x}) = \widetilde{\mathcal{V}}_{k-1}(\boldsymbol{x}) + d_k\Big(\tfrac{2\,||\boldsymbol{\gamma}(s)-\boldsymbol{x}||}{c}\Big) \cdot \exp\Big(2\pi \mathrm{i} f_\mathrm{c} \tfrac{2\,||\boldsymbol{\gamma}(s)-\boldsymbol{x}||}{c}\Big) \exp\Big(-\mathrm{i}\,\widehat{\phi}_k\Big).$$

The outcome of this proposed differential autofocus technique is the differential distance

$$r_\Delta(\boldsymbol{x}) = \frac{c}{4\pi f_\mathrm{c}} \cdot \widehat{\phi}_k$$

from flight path $\boldsymbol{\gamma}$ to the prominent points. This difference regarding a few reflectors on the ship is used to compute the distance from $\boldsymbol{\gamma}$ to all pixel in the image by linear regression. Let $X = (x_1, \ldots, x_{N_\mathrm{pix}})^\mathrm{T}$ and $Y = (y_1, \ldots, y_{N_\mathrm{pix}})^\mathrm{T}$ be the vectors, which contain the x- and y-coordinates of the image grid. Then

$$\begin{aligned} A :=& (1, x_\mathrm{pt}, y_\mathrm{pt}) \\ (\alpha, \beta, \gamma)^\mathrm{T} =& (A^\mathrm{T} A)^{-1} \cdot (A^\mathrm{T} r_\Delta) \\ \widetilde{r} =& \alpha + \beta\, X + \gamma\, Y \end{aligned}$$

gives the interpolated distance $\widetilde{r}$. Now, we have the relative distance for every pixel, which can be used in Eq. (4) for the computation of the focused ship image by Backprojection in high resolution.

VI. Simulation Results

We present the behavior of the proposed backprojection autofocus technique of moving ships by one example. A single-channel X-Band SAR system with parameters listed in Table 1 is simulated. The flight path is a straight line, which is exactly known. The simulated raw data is generated by Eq. (2). The application of the range compression in Eq. (3) yields the data, which is used for simulation.

We simulate a tanker, see Fig. 1, which has a length of 200 m and an width of 60 m. It consists of a superposition of several point reflectors. Its motion is considered as a straight linear movement added by some cosine rotations, which simulate the waves of the rough sea state. This typical ship motion [1] includes accelerations.

Table 1: Parameter of simulated X-Band SAR system.

Parameter	Value
Carrier frequency f_c	9.6 GHz
Pulse bandwidth B	200 MHz
Pulse duration T	6 μs
Sampling frequency f_s	400 MHz
Pulse repetition frequency f_{prf}	2000 Hz
Squint angle θ_S	0°
Depression angle θ_D	20°

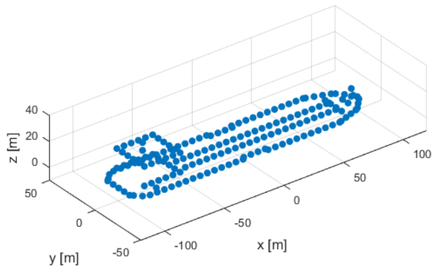

Fig. 1: Simulated ship. Each filled point is used as a point reflector to simulate synthetic data.

The following figures show the SAR image without any compensation in Fig. 2b, with a standard autofocus method from Duersch et al. [3] and Ash [4] in Fig. 2c and with our proposed ship autofous technique in Fig. 2d. It can clearly be seen, that without any autofocus technique, the type of the ship cannot be identified. The results in Fig. 2c tells us that the autofocus technique from Duersch [3] and Ash [4] yields a SAR image, where the ship can be classified as a tanker. Our autofocus method in Fig. 2d has the ability to focus the image to high quality for detailed statements. It is geometrically correct focused. The noise in the image results from non exact estimation of the position of the point reflectors.

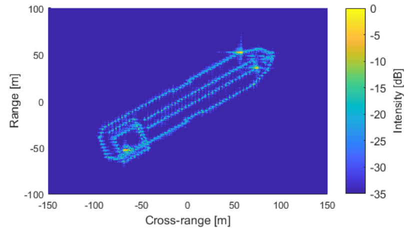

(a) Perfectly focused ship using its simulated motion

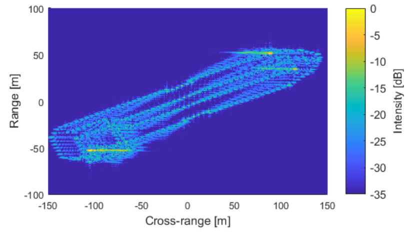

(b) Unfocused SAR image

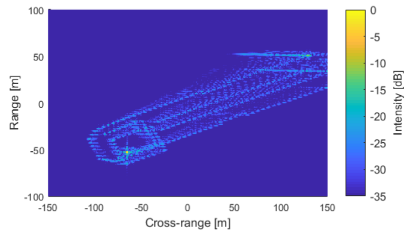

(c) Autofocus by Duersch [3] and Ash [4]

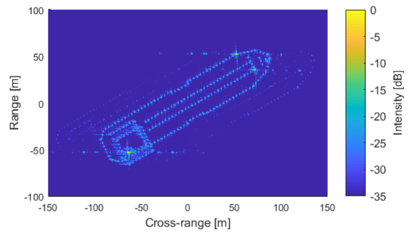

(d) Proposed autofocus method

Fig. 2: SAR images of the moving ship. In (a) the exact simulated motion is used to focus the ship perfectly. The images (b) – (d) are processed without and with autofocus.

VII. Conclusions

We present in this paper a backprojection autofocus technique, which enables the computation of sharp SAR images of moving ships. We assume that a standard ship detector, for example a CFAR detector, estimates the rough approximated position of a marine object in a preview SAR image. Our method estimates the motion, actually the rotation and the translation of the ship, which maximizes the image sharpness. Our technique might improve the results of a automatic ship classification algorithm in SAR images, which do not need AIS information.

References

[1] C. Livingstone, M. Dragosevic, S. Chu: *Ship detection and measurement of ship motion by multi-aperture Synthetic Aperture Radar*, Defence Research and Development, Scientific Report, June 2014.

[2] T. N. Hannevik, O. Olsen, A. N. Skauen, R. Olsen: *Ship detection using high resolution satellite imagery and space-based AIS*, International WaterSide Security Conference, pp. 1-6, Carrara, November 2010.

[3] M. I. Duersch, D. G. Long: *Backprojection Autofocus for Synthetic Aperture Radar*, Department of Electrical and Computer Engineering, Brigham Young University, 2013.

[4] J. N. Ash: *An Autofocus Method for Backprojection Imagery in Synthetic Aperture Radar*, IEEE Geoscience and Remote Sensing Letters, pp. 104-108, January 2012.

[5] L. A. Gorham, L. J. Moore: *SAR image formation toolbox for MATLAB*, Proc. SPIE, Vol. 7699, Algorithms for Synthetic Aperture Radar, Imagery XVII, 2010.

[6] M. Cheney, B. Borden: *Fundamentals of Radar Imaging*, SIAM, Philadelphia, 2009.

[7] I. A. Cumming, F. H. Wong "Digital Processing of Synthetic Aperture Radar Data - Algorithms and Implementation", *Artech House*, Boston, 2005.

[8] L.M.H. Ulander, H. Hellsten, G. Stenstrom, *Synthetic-Aperture Radar Processing Using Fast Factorized Back-Projection*, IEEE Transactions on Aerospace and Electronic Systems, Volume: 39, pp. 760-776, 2003.

[9] M. Richards: *Fundamentals of Radar Signal Processing*, McGraw-Hill Education, 2014.